RSC Advances

PAPER

View Article Online
View Journal | View Issue

Cite this: *RSC Adv.*, 2018, **8**, 13820

Giant magnetic coercivity in Fe_3C-filled carbon nanotubes†

Dan Liu,[a] Jie Zhu,[a] Sameera Ivaturi,[a] Yi He,[c] Shanling Wang,[c] Jiayu Wang,[a] Sijie Zhang,[ab] Maureen A. C. Willis *[ab] and Filippo S. Boi *[ab]

Received 27th December 2017
Accepted 3rd April 2018

DOI: 10.1039/c7ra13671d

rsc.li/rsc-advances

One of the major challenges in the synthesis of ferromagnetically filled carbon nanotubes is the achievement of high coercivities. Up to now the highest coercivity has been shown to be 2200 Oe at 2 K ranging down to 500 Oe at temperatures of 300 K. Here we show that the anomalously large coercivity of 3440 Oe is observed in comparable samples. By comparing our result to those reported in previous studies no correlation is found between coercivity and the shape anisotropy or the crystal-diameter. Instead we suggest that the main parameter which controls the coercivity of these structures is the interplay of the grain size and shape anisotropy. We attribute the anomalous coercivity to the grain size being below the calculated single magnetic domain limit.

Introduction

In the last decade carbon nanotubes (CNTs) have become a major focal point of nanotechnology owing to their exceptional physical, chemical and mechanical properties.[1–6] These nanostructures have been considered ideal candidates for numerous applications in the field of aerospace,[5] artificial muscles,[6] buckypaper and nano-containers or nano-capsules[7–11] in addition to many others. In particular, the use of these structures as nano-containers can allow for the protection of a desired material or crystal from the external environment since the CNT walls can chemically passivate the encapsulated material, ensuring a longer life-time.[7–20] Consequently, the encapsulation of orthorhombic, ferromagnetic Fe_3C single crystals inside CNTs has attracted much attention for their potential to possess exceptional saturation magnetizations and coercivities.[7–10,13,14,21–27] Indeed, reports have already shown that Fe_3C-filled CNT structures can reach extremely large coercivities of 2200 Oe at 2 K[13] as well as high saturation magnetization values up to 110 emu g^{-1}.[10] These properties make them particularly suitable candidates for application in data recording devices, exchange bias systems and quantum disks where high data storage densities are desired.[14] Thus far, the high coercivities of these structures have been reported to depend strongly on the shape anisotropy and crystallinity of the encapsulated crystals.[13] Furthermore, exchange bias or interactions have been reported to play an important role.[17–20] However, despite the work already carried out, the competing role of the two anisotropic parameters, namely the shape anisotropy and magnetocrystalline anisotropy on the control of the crystal coercivity has not yet been considered or understood experimentally. The investigations up till now have been focused on the theoretical aspect of the anisotropy and, to the best of the authors knowledge, whilst there has been some experimental evidence a complete experimental study for comparison to theory is yet to be performed for the interplay between the two forms of anisotropy.

Even without a full understanding of the root of such large coercivities in these materials much effort has been made to synthesise materials with higher and higher coercivities. The typical method reported in the literature generally involves ferromagnetically-filled CNTs grown on top of thermally oxidized Si/SiO_2 substrates through chemical vapour deposition (CVD) of metallocenes. Two main approaches are generally used: solid-source CVD in which an organometallic material, ferrocene,[20,21] is evaporated and pyrolyzed at high temperatures in inert gas conditions or liquid source CVD in which one or more organometallic materials are dissolved into a liquid precursor generally consisting of a hydrocarbon (toluene, *n*-chlorobenzene, *etc.*) and then used in the same manner as the solid source CVD.[7–11] The decomposed metallocene in both processes has been reported to contain Fe + H_2 + CH_4 + C_5H_6 + … species which react on the surface of the substrates to nucleate the particles from which the CNTs and single-crystal filling grow simultaneously in the form of a highly ordered film with vertical alignment.[7–11] When the precursor used is the only ferrocene, the CNTs tend to encapsulate mixed or single Fe based phases such as Fe_3C, α-Fe or γ-Fe.[17–20] In

[a]*College of Physical Science and Technology, Sino-British Materials Research Institute, Sichuan University, Chengdu, Sichuan, 610064 PR China. E-mail: m.willis@scu.edu.cn; f.boi@scu.edu.cn*

[b]*School of Physics and Astronomy, Queen Mary University of London, London, E1 4NS, UK*

[c]*Analytical and Testing Centre, Sichuan University, Chengdu, Sichuan, 610064 PR China*

† Electronic supplementary information (ESI) available. See DOI: 10.1039/c7ra13671d

order to avoid the formation of such mixed phases within the CNT capillary a post-synthesis fast-cooling step (quench) is generally used for the encapsulation of large quantities of the Fe_3C phase.[28] The chosen flow-rate of the inert gas (Ar or N_2) can also play an important role in controlling the phase-composition of the encapsulate crystals: fast flow rates of 100 ml min^{-1} have been generally reported to favour the formation of high α-Fe contents, while low vapour flow rates generally lead to the encapsulation of a higher Fe_3C content due to the higher concentration of carbon feedstock in the CVD system.[28]

In this work we employ such synthesis methods as we focus our attention on the control of the coercivity property of Fe_3C crystals encapsulated inside multiwall CNTs. In particular, we report the synthesis of single phase Fe_3C-filled CNT structures which exhibit an anomalously large coercivity of 3440 Oe, much larger than the value previously reported of 2200 Oe for the specific case of CNTs filled with the same ferromagnetic phase.[13] We show that by comparing our result to those reported in previous studies no correlation is found between coercivity and only the shape anisotropy or diameter. Instead we suggest that the main parameter which controls the coercivity of these structures is the interplay of the grain size and shape anisotropy. We demonstrate the large coercivities of these structures through SQUID magnetometry. The morphology, filling rate and crystal structure are demonstrated through scanning electron microscopy (SEM), transmission electron microscopy (TEM) and X-ray diffraction (XRD).

Results and discussion

Magnetic properties

As mentioned above high magnetic coercivities are desirable for the application of ferromagnetic-filled CNTs in exchange bias and data storage devices. With this in mind, a typical method was employed to synthesise pure, single phase Fe_3C-filled CNTs. The CNT structures were grown using solid source CVD on silicon substrates for which the full details are described in the Experimental section. Naturally, once synthesized the magnetic characteristics were measured to compare with previously reported values in literature. Fig. 1a shows the results of these measurements at 50, 100, 150 and 200 K. The first point to note is that the CNTs are ferromagnetic as expected for Fe_3C and exhibit a conventional hysteresis loop with a saturation magnetization value comparable to previously measured systems of the same material.[9] Both the saturation magnetization and coercivity can be determined for each temperature. In order to firstly understand whether a single phase of Fe_3C or multiple phases in the filling were contributing to the magnetic behaviour the saturation magnetization as a function of temperature was plotted. This is shown in Fig. 1a and the full hysteresis loops for each temperature are shown in the inset. It is immediately clear that the saturation magnetization is increasing with decreasing temperature as would be expected for a typical ferromagnetic material with no unusual behaviour which would instead be observed in presence of antiferromagnetic components like γ-Fe.[17,19]

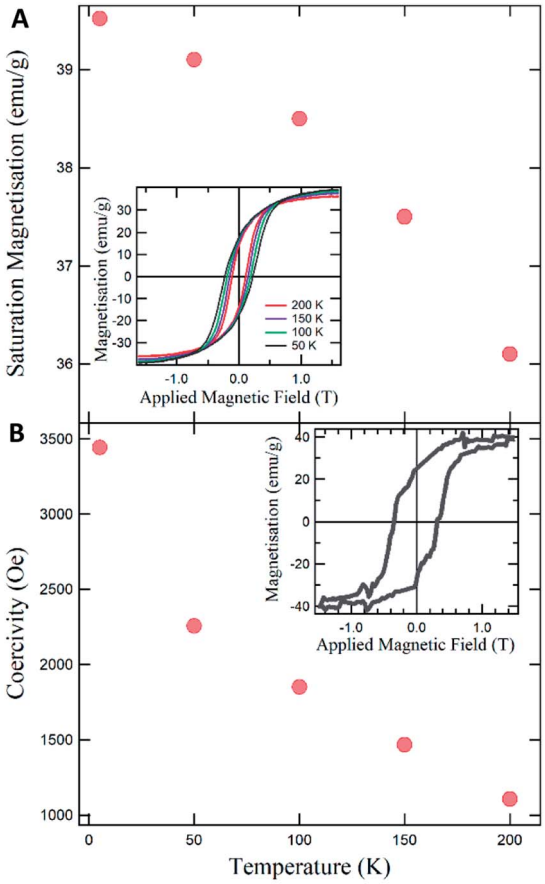

Fig. 1 (A) Saturation magnetisation as a function of temperature and full hysteresis loops (inset). (B) Coercivity as a function of temperature with full hysteresis loop for 5 K (inset).

Having established that the Fe_3C-filled CNTs synthesized appear to follow the magnetisation behaviour of those previously reported,[9] attention was turned to the more critical property – the magnetic coercivity. This is plotted as a function of temperature in Fig. 1b. Initially the coercivity at 200 K (1107 Oe) seems to match with previously reported values in these materials.[9] However, on closer investigation an interesting behavior emerges as the temperature is decreased; the coercivity increases more rapidly than in previous reports. In fact, the value at 50 K is already slightly higher (2258 Oe) than the highest reported value in these systems of 2200 Oe, which was measured at the lower temperature of 2 K.[13] This is very surprising as the materials initially appear very similar in nature and would be expected to exhibit similar behavior. To probe this increased coercivity further the value for the coercivity at 5 K was determined to directly compare with value determined at 2 K in the literature[13] (the full hysteresis at 5 K is shown in the inset of Fig. 1b). The result was even more surprising as the coercivity was significantly higher at 3440 Oe and forms the key point of the work reported here. In fact, to the best of the authors knowledge, this is the highest coercivity reported to date for Fe_3C-filled CNTs. Such a coercivity is very exciting and indeed has great promise for future application but

the source of this anomalously high value needs to be understood. Thus in the following sections the growth, morphology and structure of the synthesized CNTs are studied in more depth.

Morphology and structure

In order to understand the origin of the high coercivity SEM and TEM micrographs were taken to establish the exact morphology of the CNT systems. Fig. 2 shows the SEM micrographs at various scales for the obtained structures. The first point to notice is that the CNTs appear to be formed in ordered sections with length in the order of hundreds of microns.

On closer inspection the CNTs growth mode becomes more apparent. It can be observed that all the CNTs originate from a catalyst particle formed in a crust-like catalyst layer. This layer then breaks up after growth resulting in the ordered sections observed. The second point to notice is that the CNTs are densely packed and highly aligned in the individual sections which is desirable for data storage applications. One key point when considering the magnetic behavior however, is that despite being so densely packed, the separation between Fe_3C particles in neighboring tubes is still in the order of tens to hundreds of nanometers so one would not expect there to be a direct dipolar magnetic interaction between the particles as they are spatially too far separated. Thus, attention was then turned to the morphology and structure of the particles inside the individual tubes. Fig. 3 shows the TEM micrographs for the Fe_3C-filled CNTs.

It can be seen from micrograph A that the Fe_3C filling is not continuous along the tube. If an individual tube is focused on as in micrograph 3B two interesting points can be observed. The first is that the separation of the particles within a single tube is in the order of 50 nm at which distance a direct exchange interaction would not be expected. The second point of interest is that it is in fact possible to track the growth direction of the tubes thanks to the presence of graphene-like caps which are oriented toward the CNT-growth direction. The presence of these caps is generally observed in one type of CNT growth mechanism known as the catalyst-pool method.[29] Lastly micrograph D shows that the length and diameter of the individual particles can be determined and are important in understanding the role of the anisotropy discussed later. A further, more detailed HRTEM image along with its electron

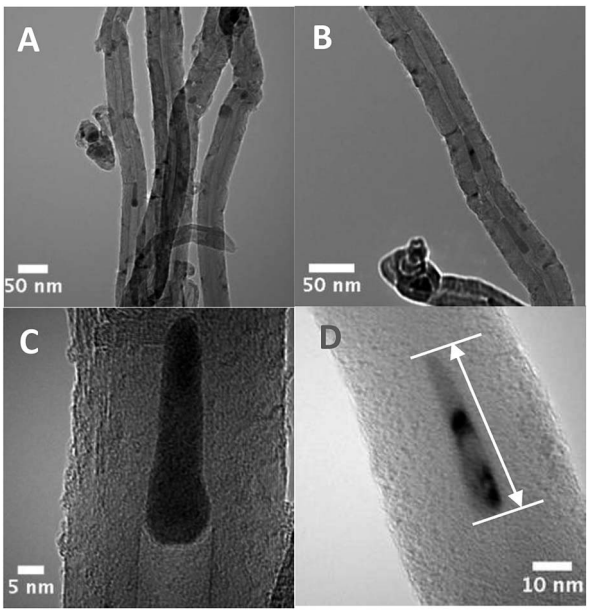

Fig. 3 TEM micrographs showing in (A) the typical cross-sectional morphology of the carbon nanotubes with an average diameter of approximately ~50 nm. In (B–D) typical examples of encapsulated particles are shown. Graphene like caps were also observed and suggest the presence of a catalyst-pool growth mechanism.

diffraction pattern can be seen in Fig. S-1† confirming the crystallinity of the filling. Since the morphology of the system offers no clear explanation for the anomalously high coercivity, further investigations were performed on the structure and phases of the nanowires. As mentioned earlier the presence of two Fe-based phases within the same nanowire can result in additional magnetic interactions in presence of direct physical contact or if the conditions are correct such as the interaction distance. Fig. 4 shows a typical example of the powder X-ray diffractogram obtained for the produced sample.

In particular, the Rietveld refinement was used to assign the observed peaks to the right Fe-based phase. The refinement and the baseline are shown by the solid red and green lines

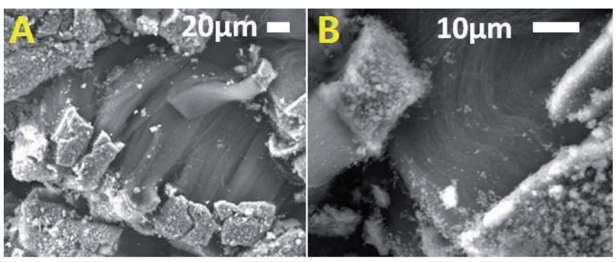

Fig. 2 Typical SEM micrographs showing the morphological quality of the as grown CNTs films. Notice the presence of a catalyst layer on the bottom of the film.

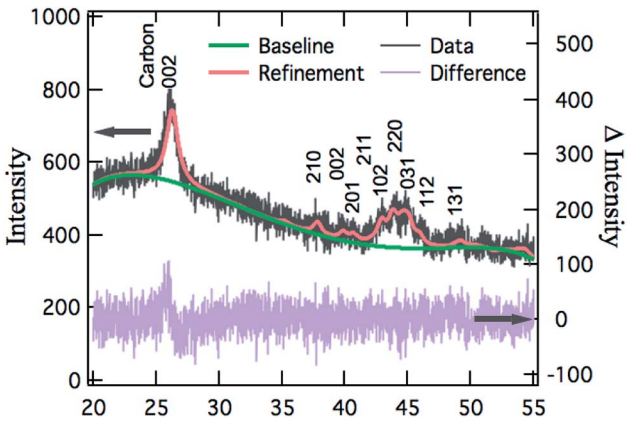

Fig. 4 XRD diffractogram and Rietveld refinement of the as grown sample showing the presence of a single crystalline phase of Fe_3C.

respectively along with the peak assignments in Fig. 4. It immediately becomes clear that, whilst there is some preferred orientation present, thus accounting for the slight differences in the fitted and actual peak amplitudes, the filling consists of only a single Fe_3C phase with space group *Pnma* (database card 1008725 extracted from the Crystallography Open COD database). This agrees with the saturation magnetization data presented earlier which demonstrated no unusual features with temperature. In addition, XPS measurements (ESI Fig. S-2†) confirm only the presence of Fe and C as the main contribution. Thus, we can conclude that the morphology and structure of the Fe_3C-filled CNTs reported here are consistent with previously reported systems of a similar nature and are consequently not expected to be the direct cause of any high coercivity.

Size, shape and anisotropy

As introduced earlier there have been some previous studies that strongly correlate the change in the dimensions or shape anisotropy to the change in coercivity in these materials. Up till now these studies have focused on the physical size of the elongated particles also referred to as nanowires. One key study was that by A. Morelós-Gómez *et al.* who performed in-depth simulations of the result of changes in diameter and the aspect ratio on the coercivity in ferromagnetic nanowires encapsulated in carbon nanotubes.[13] They show with experimental and theoretical studies how it is possible to control the coercivity to high values by reducing the diameter of the wire/particle. It is concluded that highly aligned nanowires with dimensions in the order of 5 nm diameter by 25 nm length should be achieved to obtain high coercivities suitable for device application. They also conclude that the aspect ratio of the wire is not significant in controlling the coercivity. Consequently, to ascertain how the size and shape of the particles in the CNTs reported here are influencing the coercivity, we determined the statistical distribution of the diameter and length of 174 different particles from the TEM micrographs. Fig. 5 shows the resultant histograms for both the diameter and length of the particles.

The first point to note is that the distribution is reasonably central and has a FWHM of around 5 nm. The second point to note is that the diameter of the particles is in the order of 9 nm and the length is around 35 nm which is directly comparable to the diameter and length of the nanowires produced in the aforementioned study.[13] Given that the morphology, structure and size of the encapsulated Fe_3C crystals are the same then it remains curious as to why the coercivity is so much higher than the values reported in literature. Following the idea of A. Morelós-Gómez *et al.*[13] that the diameter of the nanowire (for a fixed length of 80 nm) is the key factor, then in order to achieve the values reported here, the diameter would have to be smaller than 5 nm. This is roughly a factor of two less than that measured from the TEM micrographs. Thus the diameter alone cannot be considered the key factor for the high coercivity reported here.

One must then consider both the shape and magneto-crystalline anisotropy of the particles. In this case the former would not be expected to play a significant role as whilst the particles are narrow, the average length is only in the order of 35 nm providing an aspect ratio of just under 4. This aspect ratio is not dissimilar to the previously reported cases which also do not show such a high coercivity resulting from the aspect ratio. In fact, for the average diameter in this work, reducing the length from around 70 nm to 40 nm has been shown to decrease the coercivity, which corresponds with the idea that the shape anisotropy is reduced. We thus consider the magneto-crystalline anisotropy and any effects resulting from the grain size of the Fe_3C. The average grain size was determined from the XRD peak width to be 7.2 nm. This is typically very small and is well in the size range of single domain and even paramagnetic particles.

It is possible to calculate the upper single domain limit in such systems and several discussions on the different methods are published in the literature. The calculation shown here was performed using eqn (1) from the report of Blundell:[30]

$$r_{Fe_3C} < \frac{9\pi\sqrt{A(K_{sa} - K_{ma})}}{\mu_0 {M_s}^2} \quad (1)$$

here K_{sa} is the shape anisotropy energy density of an elongated Fe_3C ellipsoid of revolution (0.3×10^6 J m^{-3}), K_{ma} is the magnetocrystalline anisotropy energy density of an elongated Fe_3C ($K_1^{ma} = 0.394 \times 10^6$ J m^{-3} and $K_2^{ma} = 1.88 \times 10^5$ J m^{-3}) ellipsoid of revolution, M_s is the saturation magnetization (9.8×10^5 A m^{-1} for Fe_3C) and A is the exchange stiffness constant that is 8.7×10^{-12} J m^{-1} for Fe_3C.[30–34] The exchange stiffness constant can be written as shown in eqn (2):[26,27,30–32]

$$A = \frac{2JS^2z}{a} \quad (2)$$

where J is the exchange integral, a is the nearest neighbour distance, z is the number of sites in the unit cell ($z = 2$ for body centered cubic) and S the spin.[30] The critical radius value determined for the slightly elongated Fe_3C particles in this study was 23 nm. A key point to note in this calculation is that the shape anisotropy is accounted for by taking the difference between the two anisotropy energy coefficients. The question then remains if there is any presence of superparamagnetism. Nominally one would expect a collapse in coercivity above the blocking temperature in the superparamagnetic particles, resulting from spins being able to flip with ease between the different magnetisation axis. This is then frozen out below the

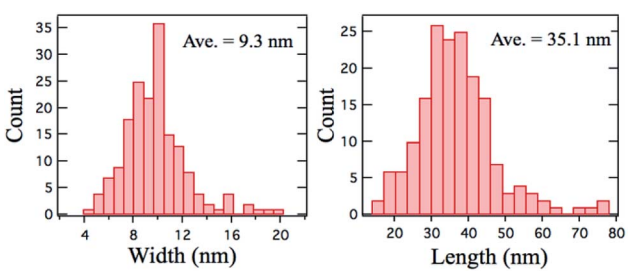

Fig. 5 Statistical distribution of diameter and length of the encapsulated Fe_3C crystals.

blocking temperature. Although no such collapse is seen in the coercivity, the squareness factor (ESI Fig. S-3†) and magnetisation behaviour as well as the increased coercivity with temperature are comparable with recent studies where this behaviour is indicative of superparamagnetism.[33] The critical value of the squareness factor reported for superparamagnetic systems in literature is 0.5,[34] which is consistent with the values obtained from the hysteresis curves measured here (0.38 at 200 K to 0.62 at 5 K). The lack of collapse can be understood if one considers the distribution of the particle size. The variation can result in only a small percentage of the particles being in the superparamagnetic regime. The magnetic properties would then be expected to be limited by the largest particle size. Thus, it is possible that the particle size is at the limit between single domain and superparamagnetic behaviour.

Experimental

200–300 mg of decamethyl-cyclopentadienyl-iron was evaporated ($T = 300$ °C) and pyrolyzed ($T = 900$ °C at the reaction deposition) in a CVD reactor consisting of a quartz-tube of 1.5 m, outer diameter of 22 mm and wall thickness of 2.5 mm and a tube furnace set at the temperature of 990 °C. The Ar flow rate was 10–15 ml min^{-1}. The characterisation was performed using: (1) SEM with a JSM-7500F at 5–20 kV. (2) TEM with a 200 kV American FEI Tecnai G2F20. (3) XRD with a Empyrean Panalytical (S/N: DY1588, Cu K-α source with lambda = 0.154 nm), with 0.013° per step and 30 s as time per step. (4) A Squid Quantum Design was used for the magnetic characterization.

Conclusions

Here we have synthesised Fe_3C-filled CNTs using a standard CVD approach. The magnetic behaviour and morphology, size and structure are measured for the Fe_3C particles formed. Interestingly an anomalous coercivity, higher than any previously reported for this material, of 3440 Oe is observed. It is shown that the diameter and shape anisotropy alone are not sufficient to explain such a high value and further explanation is required. The grain size and particle size were determined and compared to the calculated single domain critical radius. Considering this and the behaviour of the squareness factor, magnetisation and coercivity with temperature it is concluded that the anomalous values can quite possibly originate from single domain and even superparamagnetic behaviour. Given the high coercivity and alignment of the CNTs, these results are extremely promising for future applications in data storage.

Conflicts of interest

There are no conflicts to declare.

Acknowledgements

We acknowledge funding from the NSCF (grant numbers: 11404227, 61574095 and 61307039).

Notes and references

1 S. Iijima, *Nature*, 1991, **354**, 56.
2 S. Iijima and T. Ichihashi, *Nature*, 1993, **363**, 603.
3 M. Oberlin, A. Endo and T. Koyama, *J. Cryst. Growth*, 1976, **32**, 335.
4 L. V. Radushkevich and V. M. Lukyanovich, *Zurn. Fisic. Chim.*, 1952, **26**, 88.
5 M. S. Dresselhaus, *Nat. Mater.*, 2004, **3**, 665.
6 U. Vohrer, M. H. Haque, S. Roth and U. Detla-Weglikowska, *Carbon*, 2004, **42**, 1159.
7 J. Guo, Y. He, S. Wang and F. S. Boi, *Carbon*, 2016, **102**, 372.
8 F. S. Boi, J. Guo, S. Wang, Y. He, G. Xiang, S. Zhang and M. Baxendale, *Chem. Commun.*, 2016, **52**, 4195.
9 R. Lv, S. Tsuge, X. Gui, K. Takai, F. Kang, T. Enoki, J. Wei, J. Gu, K. Wang and D. Wu, *Carbon*, 2009, **47**, 1141.
10 J. Guo, M. Lan, S. Wang, Y. He, S. Zhang, G. Xiang and F. S. Boi, *Phys. Chem. Chem. Phys.*, 2015, **17**, 18159.
11 X. Gui, J. Wei, K. Wang, W. Wang, R. Lv, J. Chang, F. Kang, J. Gu and D. Wu, *Mater. Res. Bull.*, 2008, **43**, 3441.
12 T. Peci and M. Baxendale, *Carbon*, 2015, **98**, 519.
13 A. Morelós-Gómez, F. Lopez-Urias, E. Munoz Sandoval, C. L. Dennis, R. D. Shull, H. Terrones and M. Terrones, *J. Mater. Chem.*, 2010, **20**, 5906.
14 H. Terrones, F. Lopez-Urias, E. Munoz Sandoval, J. A. Rodriguez-Manzo, A. Zamudio, A. L. Elias and M. Terrones, *Solid State Sci.*, 2006, **8**, 303.
15 A. Leonhardt, M. Ritschel, R. Kozhuharova, A. Graff, T. Muhl, R. Huhle, I. Monch, D. Elefant and C. M. Schneider, *Diamond Relat. Mater.*, 2003, **12**, 790.
16 F. C. Dillon, A. Bajpai, A. Koos, S. Downes, Z. Aslam and N. Grobert, *Carbon*, 2012, **50**, 262.
17 C. Prados, P. Crespo, J. M. Gonzalez, A. Hernando, J. F. Marco, R. Gancedo, N. Grobert, M. Terrones, R. M. Walton and H. W. Kroto, *Phys. Rev. B: Condens. Matter Mater. Phys.*, 2002, **65**, 113405.
18 J. F. Marco, J. R. Gancedo, A. Hernando, P. Crespo, C. Prados, J. M. Gonzalez, N. Grobert, M. Terrones, D. R. M. Walton and H. W. Kroto, *Hyperfine Interact.*, 2002, **139**, 535.
19 F. S. Boi, G. Mountjoy and M. Baxendale, *Carbon*, 2013, **64**, 516.
20 S. Karmakar, S. M. Sharma, M. D. Mukadam, S. M. Yusuf and A. K. Sood, *J. Appl. Physiol.*, 2005, **97**, 054306.
21 D. Golberg, M. Mitome, C. Muller, C. Tang, A. Leonhardt and Y. Bando, *Acta Mater.*, 2006, **54**, 56.
22 C. Muller, D. Golberg, A. Leonhardt, S. Hampel and B. Buchner, *Phys. Status Solidi A*, 2006, **203**, 1064.
23 S. Hampel, A. Leonhardt, D. Selbmann, K. Biedermann, D. Elefant, C. Muller, T. Gemming and B. Buchner, *Carbon*, 2006, **44**, 2316.
24 A. K. Schaper, H. Hou, A. Greiner and F. Phillipp, *J. Catal.*, 2004, **222**, 250.
25 U. Weissker, M. Loffler, F. Wolny, M. U. Lutz, N. Scheerbaum, R. Klingeler, T. Gemming, T. Muhl, A. Leonhardt and B. Buchner, *J. Appl. Physiol.*, 2009, **106**, 054909.

26 M. U. Lutz, U. Weissker, F. Wolny, C. Muller, M. Loffler, T. Muhl, A. Leonhardt, B. Buchner and R. Klingeler, *J. Phys.: Conf. Ser.*, 2010, **200**, 072062.
27 F. S. Boi, S. Maugeri, J. Guo, M. Lan, S. Wang, J. Wen, G. Mountjoy, M. Baxendale, G. Nevill, R. Wilson, Y. He, S. Zhang and G. Xiang, *Appl. Phys. Lett.*, 2014, **105**, 243108.
28 A. Leonhardt, M. Ritschel, D. Elefant, N. Mattern, K. Biedermann, S. Hampel, C. Muller, T. Gemming and B. Buchner, *J. Appl. Physiol.*, 2005, **98**, 074315.
29 R. Xiang, G. Luo, W. Qian, Q. Zhang, Y. Wang, F. Wei, Q. Li and A. Cao, *Adv. Mater.*, 2007, **19**, 2360.
30 S. Blundell, *Magnetism in Condensed Matter*, Oxford University Press, 2001.
31 K. D. Sattler, *Principles and Methods*, CRC Press, 2011.
32 M. Getzlaff, *Fundamentals of Magnetism*, Springer, 2008.
33 K. Lipert, J. Kazmierczak, I. Pelech, U. Narkiewicz, A. Slawska-Waniewska and H. K. Lachowicz, *Mater. Sci.-Pol.*, 2007, **25**, 2.
34 E. C. Stoner and E. P. Wohlfarth, *Philos. Trans. R. Soc. London, Ser. A*, 1948, **240**, 599.